Open Access

Research Article

PRNANO

Prec. Nanomed. 2018 Oct;1(3):197-210.

ANDOVER HOUSE

Specific Molecular Recognition as a Strategy to Delineate Tumor Margin Using Topically Applied Fluorescence Embedded Nanoparticles

Shawn Barton[2], Bo Li[2], Michael Siuta[2], Vaibhav A Janve[2], Jessica Song[2], Clinton M. Holt[2], Takumi Tomono[1], Masami Ukawa[1], Hironori Kumagai[3], Etsuo Tobita[3], Kevin Wilson[2], Shinji Sakuma[1*] and Wellington Pham[5, 7, 8, 9, 10, 121]

[1]*Faculty of Pharmaceutical Sciences, Setsunan University, Hirakata, Osaka, Japan*
[2]*Vanderbilt University Institute of Imaging Science, Nashville, TN*
[3]*Life Science Materials Laboratory, ADEKA Corp., Tokyo, Japan*
[4]*Department of Radiology and Radiological Sciences, Vanderbilt University, Nashville, TN*
[5]*Department of Biomedical Engineering, Vanderbilt University, Nashville, TN*
[6]*Vanderbilt Ingram Cancer Center, Vanderbilt School of Medicine Nashville, TN*
[7]*Vanderbilt Brain Institute, Nashville, Vanderbilt University, TN*
[8]*Vanderbilt Institute of Chemical Biology, Nashville, TN*

Submitted: July 18, 2018 Accepted: October 27, 2018

GRAPHICAL ABSTRACT

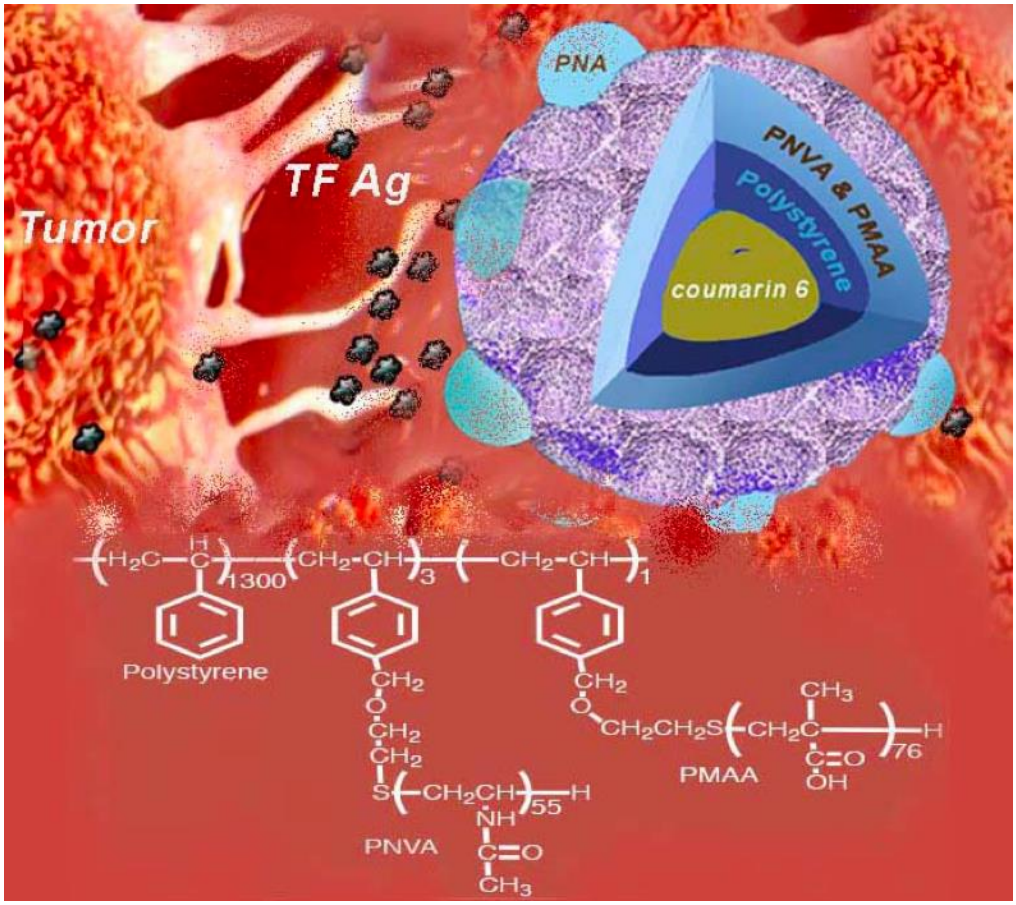

[1] Corresponding authors: Wellington Pham, Vanderbilt University Institute of Imaging Science, 1161, 21st Avenue South, AAA 3117, Nashville, TN 37232. wellington.pham@vanderbilt.edu, Tel. : 615-936-7621; Fax: +1-615-322-0734; Shinji Sakuma, Faculty of Pharmaceutical Sciences, Setsunan University, 45-1 Nagaotoge-cho, Hirakata, Osaka 573-0101, Japan, sakuma@pharm.setsunan.ac.jp, Tel.: +81-72-866-3124; Fax: +81-72-807-6078

ABSTRACT

The Thomsen-Friedenreich (TF) antigen is a tumor-associated antigen consistently expressed on the apical surface of epithelial-based cancer cells, including pancreatic cancer. In this work, we report the development of a multimodal imaging probe, the tripolymer fluorescent nanospheres, whose surface was fabricated with peanut agglutinin (PNA) moieties as TF molecular recognition molecules. Here, we demonstrate that the probe is able to detect TF antigen in human pancreatic cancer tissues and differentiate from normal tissue. What is most noteworthy regarding the probe is its ability to visualize tumor margins defined by epithelial TF antigen expression. Further, in vivo preclinical studies using an orthotopic mouse model of pancreatic cancer suggest the potential use of the nanospheres for laparoscopic imaging of pancreatic cancer tumor margins to enhance surgical resection and improve clinical outcomes.

Keywords:

- TF antigen,
- tumor margin,
- pancreatic cancer,
- nanotechnology

Abbreviations:

- TF: Thomsen-Friedenreich
- PNA: peanut agglutinin
- TFNS: tripolymer fluorescence nanospheres

RATIONALE AND PURPOSE

This project employs the multivalency and special nanoscale physics of nanotechnology to generate versatile tripolymer fluorescent nanospheres for delineation of pancreatic tumor margin. Application of optical imaging in combined with laparoscopic surgery offers better resection of tumors and improve prognosis following surgical resection.

INTRODUCTION

Pancreatic cancer accounts for approximately 7% of all cancer deaths[1], and is one of the most frequent malignant tumors[2]. The causes of pancreatic cancer are still unknown, although certain risk factors have been identified, including cigarette smoking, genetics, diabetes mellitus, obesity, dietary factors, alcohol addictions and physical inactivity[3-7]. As the response of this cancer to chemo- and radiotherapy is limited[8], more than half of all pancreatic cancers are diagnosed at stage IV and surgical resection is the patient's only hope for cure[9-10]. Although the median survival for patients undergoing resection is greater than that of patients undergoing radiochemo-therapy[11], intraoperative delineation of tumor margins is still a challenge in regard to establishing complete tumor clearance with negative margins. Apart from the anatomical complexity of the pancreas and technically demanding surgical procedure due to its location, which is adjacent to many critical organs and vascular structures[10], the highly dispersed, discontinuous growth that is characteristic of pancreatobiliary cancer further contributes to the difficulty of identifying the tumor periphery[8]. With naked-eye inspection being unreliable in detecting these discontinuous growths; failure to confirm the tumor margin during dissection will inevitably lead to under or over estimation of margin involvement[12]. These drawbacks have necessitated the development of new methods to improve clinical outcomes. One such new method is fluorescent laparoscopy, where nanotechnology is integrated with a pre-existing clinical technique in order to better decipher tumor margin during resection.

With the advent of targeted molecular imaging technology, the detection of tumor biomarkers serves as an ideal approach for the delineation of the tumor margin. Particularly for the case of pancreatic cancer dissection, survival relies on accurate and timely assessment of tumor margins during surgery. We described herein our strategy to develop a trimodal nanotechnology-based approach

involving the encapsulation, surface fabrication and block copolymerization processes for potential use as a fluorescent contrast agent to visualize pancreatic cancer margins. One tumor antigen that we are interested in testing for pancreatic cancer is the Thomsen-Friedenreich (TF) antigen. TF consists of a type I core of O-linked oligosaccharide constituents of mucins[13]. In epithelial cells, the TF is carried by mucin-1 (MUC1) on the apical surface. In tumor cells, MUC1 is post-translationally modified resulting in aberrant O-glycosylation, such as TF, a well-defined antigen with a proven link to epithelial-based carcinomas but not in normal tissues[14-15], including bladder[16], colorectal[17], gastrointestinal[18], prostate[19-20], ovarian[21], lung[22], and pancreatic[23-25] carcinomas. The TF antigen is most noteworthy for its overexpression in tumors at a rate far more frequent than for other oncogene products, such as myc, rasK or HER2/neu, and it has a greater correlation with tumor progress than that of tumor-suppressing genes such as p53 or p16 [26]. Different from other cancer imaging targets that require targeting agents to remain intact through systemic delivery, TF expression is found on the surface of epithelial cells, thus localized, topical delivery can be implemented to improve the efficiency of the targeting agent. In addition, its substantially large size and accessibility at the cell surface coupled with the occurrence of tandem repeated regions (as most TF disaccharides are expressed on the tandem repeated MUC1 protein backbone) help to amplify the targeting signal. Overall, it seems reasonably certain that high expression of TF in cancer and its absence from normal tissue represents a unique association in cancer that exhibits the qualities of a tumor margin biomarker.

The tripolymer fluorescent nanospheres (TFNS) described in this project are comprised of polystyrene nanoparticles that have coumarin 6 dyes encapsulated within the core of the nanoparticles during the co-assembly of main polymer and coating polymers during block polymerization process. Among the coating polymers, polymethacrylic acid (PMAA) provides free carboxylic groups as handles for bioconjugation with the molecular recognition moieties for targeted imaging. In this case we used peanut agglutinin (PNA) proteins, which are already known for having a high binding affinity for TF antigens[27]. In keeping with this unique PNA-TF association, developing a fundamental understanding of the in vivo expression of the TF antigen would yield strategies to achieve an effective means of detecting pancreatic cancer. Most practically, in the case of pancreatic cancer, the TFNS could serve to delineate tumor margins to assist during intraoperative tumor dissection.

In this paper we address the development of TFNS for delineating pancreatic tumor margin using human pancreatic cancer specimens in a preclinical setting, wherein the probe was able to discern normal from pathological tissues. Particularly, TF expression is not only strong in cancer tissues, its absence in normal tissues reflected by the fluorescence (FL) signal of the TFNS and in the immunoprecipitation assay make it an ideal candidate to delineate tumor margin in future clinical studies. Further, an in vivo study using an orthotopic animal model of pancreatic cancer confirmed the specificity of the probe.

EXPERIMENTAL DESIGN

This work focuses on the integration of multimodal nanotechnology with fluorescence technique and biomarker imaging for the delineation of tumor margins. The experimental protocols include the design and development a robust and reproducible chemistry for the synthesis of the TFNS probe, followed by using state-of-the-art technologies to characterize the physical property of the probe. Next, we assessed the specificity of the probe on human pancreatic specimens and an orthotopic mouse model of pancreatic cancer employing molecular imaging and molecular biology and quantitative analysis. The laboratory mice are an ideal model system for the studies proposed. Testing the binding specificity of the probe to delineate tumor margins is a very complicated process and cannot be adequately simulated in vitro. Mice are the lowest vertebrates developmentally, in which the proposed study can be conducted. In addition, the small size of these animals allows for relatively cost-effective housing and suitable equipment, such as the imaging systems and others are already available. In addition, the goal of this study is to perform binding specificity of the probes in vivo to allow insights into propagating this technology to human applications.

MATERIALS AND METHODS

Chemicals

Coumarin 6 and PNA were obtained from Sigma-Aldrich while N-vinylacetamide (NVA) monomers were kindly provided by Showa Denko Co. (Tokyo, Japan) as a gift. Allyl 2-bromoisobutyrate (ABIB), methyl ethyl ketone (MEK) and Boc-methacrylic acid (BMA) were obtained from Sigma Aldrich. All other chemicals were obtained from commercial sources at reagent grade and used without further purification. The anti-human TF monoclonal antibody was obtained from Abcam and Lifespan Biosciences.

Cell Lines

Murine pancreatic cancer cells CRL2460 were obtained from ATCC (Manassas, VA) and maintained according to the supplier's instructions.

Animal Models

Wild type C57BL/6 mice were acquired from the Jackson Laboratory. All experimental protocols were approved by the Vanderbilt University Institutional Animal Care and Use Committee.

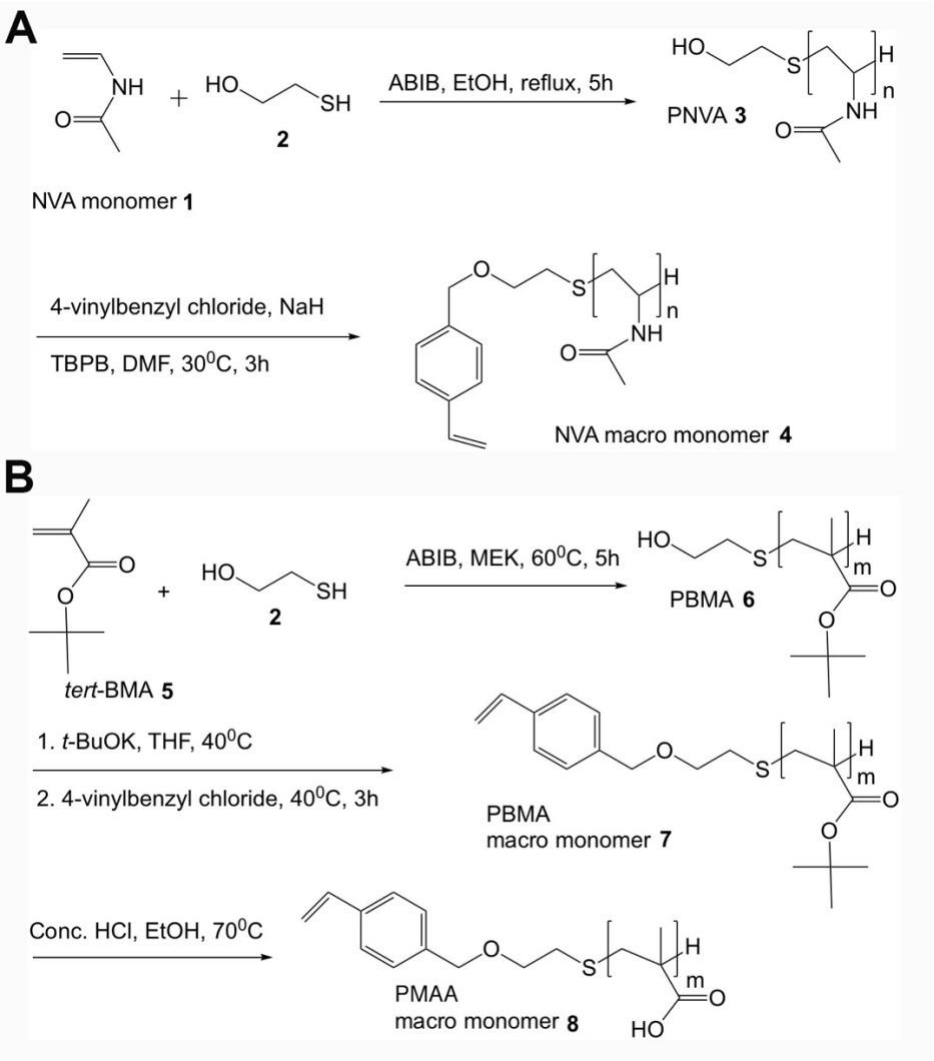

Figure 1. *Chemical modifications of the coating polymers. N-vinyl acetamide* ***1*** *was treated with mercaptoethanol in the presence of ABIB to generate PNVA* ***3****, followed by an SN2 alkylation reaction to attach the styrene moiety in anhydrous condition to afford NVA macro monomer* ***4b*** *(A); tert-BMA* ***5*** *was treated with mercaptoethanol in the presence of ABIB in MEK to generate PBMA* ***6****, followed by an SN2 alkylation reaction to attach to styrene moiety to afford PBMA macro monomer* ***7****. Cleavage of the protecting group was achieved via conventional treatment of* ***7*** *with concentrated HCl at elevated temperature to provide* ***8****.*

Synthesis of precursor polymers.

NVA macromonomer.

In a flame-dried round bottom flask purged with nitrogen, ABIB (5.43g, 2.0x10^{-2} mmol) was added to a stirring solution of non-ionic N-vinyl acetamide (200g, 2.35 mol) and 2-mercaptoethanol (92g, 1.18 mol) in ethanol, followed by heating to reflux at 70°C for 5 hours (Fig. 1A). Then the reaction was quenched by addition of ethanol (202 mL) to afford PNVA after purification torovide 33.1 g, 16 % yield.

Next, PNVA (25g) was treated with 4-vinylbenzyl chloride (13.8g, 9.0x10^{-2} mol) and NaH (3.19g, 0.16 mol), tetrabutylphosphonium bromide (TBPB) (2.8g, 1.0x10^{-2} mol) in DMF. Then, the reaction solution was slightly heated to 30°C for 3 hours followed by the reaction being quenched using ethanol. The crude product was collected by precipitation in acetone. Finally, the product was purified by dialysis in water to afford the product (13.9g, 56% yield).

PMA Macromonomer.

In a flame-dried round bottom flask purged with nitrogen, mercaptoethanol (0.58g, 7.4 x 10^{-3} mol) and ABIB (1.53g, 6.6 x 10^{-3} mol) were added to a solution of *tert*-BMA (150g, 1.05 mol) in MEK at rt and the reaction was stirred for 5 hours at 60°C (Fig. 1B). Finally, the PBMA product was collected by reprecipitation in methanol:water (1:1 v/v).

Potassium *tert*-butoxide (5.84g, 5.21 x10^{-2} mol) was added to a solution of PBMA (60g) in anhydrous THF and then the reaction solution was warmed up to 40°C followed by the addition of 4-vinylbenzyl chloride (1.93g, 1.30x10^{-2} mol), and the reaction was stirred at 40°C for 3hours. The product of PBMA macromonomer was collected by reprecipitation in a mixture of methanol and water (1:1 v/v) to afford 45.9g in 77% yield. The protecting Boc group was removed by addition of PBMA macromonomer in concentrated HCl in ethanol at 70°C to afford the desired product at 37% yield.

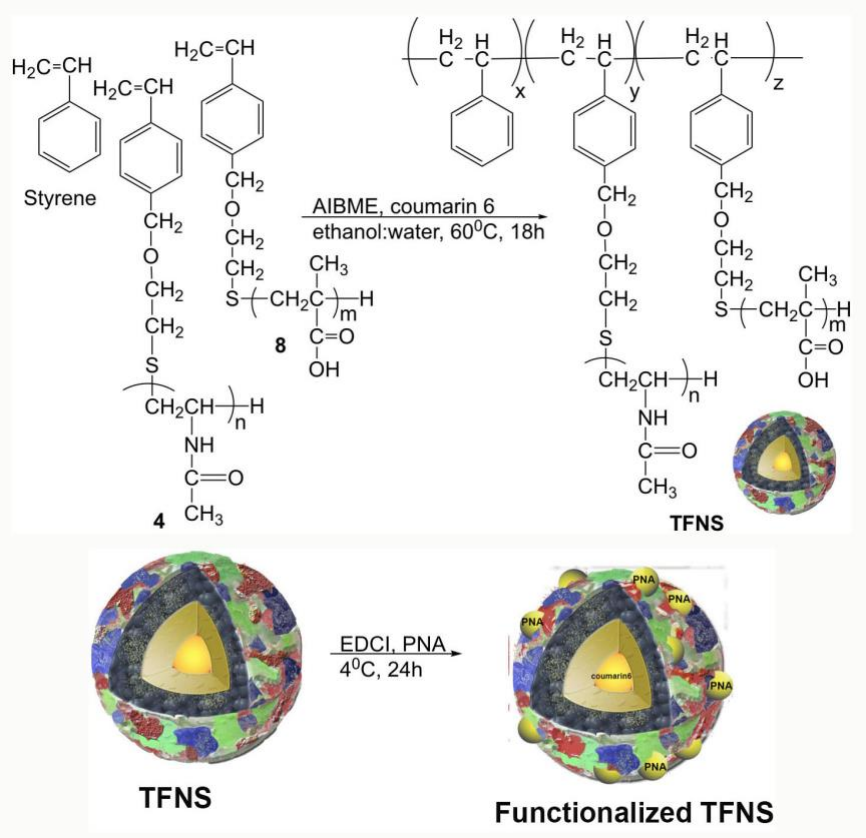

Figure 2. *Assembly of the TFNS nanoparticles through copolymerization process. Styrene along with coating polymers* ***4*** *and* ***8*** *were treated with AIBME in a mixture of ethanol and water in the presence of coumarin 6 dyes. The reaction mixture was then elevated from room temperature to 60 ℃ to provide TFNS nanoparticles, which will then be functionalized with PNA on the surface using coupling reagent EDCI.*

Preparation of PNA-laden tripolymer fluorescent nanospheres (TFNS).

To make the TFNS, NVA macromonomer **4** (1.0 eq. in grams), PMAA macromonomer **8** (1.0 eq.) and styrene (2.0 eq.) were introduced into a solution of American Institute of Biological and Medical Engineering (AIBME) (2,2'-azobis(2-methylpropionate)) (~ 1.0 mol% of the total monomers) and coumarin 6 dye (0.1% of the total monomers) in ethanol:water (2:1 ratio) (Fig. 2).

The resulting mixture was stirred for 18h at 60°C. The final product was collected by centrifugation; while, the unreacted materials were discarded in the supernatant. The product was further centrifuged repeatedly several times with an excess amount of water to remove ethanol. Finally, the TFNS nanoparticles were dispersed in ddH_2O and lyophilized for future use.

Nanocoating and pharmaceutical formulations.

The TFNS nanoparticles (20 mg/mL) were functionalized and formulated for biological studies by treating with a water-soluble coupling reagent EDCI (1-ethyl-3-(3-dimethylaminopropyl)carbodiimide) (3 equivalent) followed by addition of peanut agglutinin (PNA); the reaction was stirred for 24 hours at 4°C (Fig. 2). Then, the PNA-laden TFNS dispersion was centrifuged to separate the precipitated product from the unreacted materials (x3), and the product was finally dispersed in double distilled water. Several batches of the PNA-coated TFNS nanoparticles were synthesized using the same procedure noted previously and characterized to ensure the reproducibility of our production chemistry. All TFNS batches have a concentration of 20 mg/mL in PBS at pH 7.2 ± 0.05, and all of the physicochemical properties of the probes were confirmed in each batch of syntheses.

Super-resolution fluorescence microscopy.

Super-resolution microscopy of coverslip-mounted TFNS nanospheres were performed on ZEISS LSM 880 (Carl ZEISS, Germany) confocal laser scanning airy scan mode using Plan-Apochromat 63X/1.4 numerical aperture (N.A.) oil objective. Coumarin 6-associated TFNS nanospheres were excited with a 488 nm argon laser at 0.9% laser intensity (LI) settings and detection range centered on 523 nm. Both 2D and 3D imaging were performed and images were processed in Zen (Carl ZEISS, Germany) acquisition software with Airyscan processing and a scanning resolution of 0.04µm x 0.04µm x 0.19µm per pixel. Line profiles were evaluated and fluorescent shell diameter was calculated. Airy scan mode uses a hexagonal 32 GaAsP detector array[28-29] with each detector functioning as a small pinhole. The unique geometry allows collection of high frequency information and more light thus simultaneously improving resolution, and signal-to-noise ratio (SNR) achieving 1.7x higher resolution compared to CLSM (~130 nm in xy-plane).

Frozen tissues and imaging process.

Frozen normal and pancreatic samples were air dried and fixed with 4% paraformaldehyde for 10 minutes before exposure to a solution of citric acid buffer (pH 6.0). Then, the slides were washed with Dulbecco's phosphate buffer saline (DPBS) before exposure to the probe (2 mg/mL) for fluorescence microscopy (Nuance FX, CRI). A FITC channel was used to detect the fluorescence signal of coumarin 6 dyes emanated from the TFNS nanoparticles. Images observed under fluorescence/white visible light were captured with a CCD camera operated via Nuance software.

Luciferase transfection.

After amplification of plasmids in DH5a cells, transfection was performed in CRL-2460 cells (ATCC), the procedure was as described elsewhere, in brief: 80% confluent CRL-2460 cells (ATCC) were cultured in 6-well plate in RPMI 1640 medium supplemented with 10% fetal bovine serum and 1% penicillin/streptomycin in a 37^0C incubator with 5% CO_2. 2.5 µg plasmid DNA (pGL3 control, pSV2-neo) was mixed with Lipofectamine 2000 (ThermoFisher Scientific, Cat:11668027) at 1:2 ration (1 µg : 2 µl) in 150 µl serum-free Opti-MEM (ThermoFisher Scientific, Cat:11058021). The mixture was then incubated at room temperature for 30 minutes and then added to the above cell culture in 2 mL of fresh culture medium. The medium was replaced in 6 hours, placed back in the incubator, then medium was again replaced in 48 hours, and G418 was added at 400 µl/mL for 7 to 10 days. The culture medium with G418

was replaced in every 3 days. The final selection of cell culture was confirmed on a Xenogen IVIS 200 system with adding of D-luciferin (Gold Biotechnology, Cat: LUCK-1G) in a 24-well culture medium at 100 µg/mL. The luciferase-expressing CRL-2460 cells were either stored in liquid nitrogen or cultured in RPMI 1640 with 200 µg/mL of G418.

Immunoprecipitation and Western Blot Analysis.

Human pancreatic tissues were minced for protein extraction using T-Per Tissue Protein Extraction Reagent (ThermoFisher, 78510). The tissue was briefly sonicated on ice (30s, 20KHz) followed by protein extraction by centrifugation and the concentration was determined by BCA methods (ThermoFisher Scientific). For immunoprecipitation, the protein was precleared with Protein L Agarose beads (ThermoScientific) and vortexed at room temperature for 1hour followed by incubation with anti-TF antibodies for 15 hours at 4°C and precipitated by using Protein L Agarose beads. Beads were washed three times with IP buffer and then mixed with 2x Laemmli sample buffer. Western blotting was performed as described in the literature[30] using 8% SDS-PAGE gel and anti-TF antibody (1:300 dilution) along with HRP-conjugated anti-IgM antibodies at 1:5000 dilution.

Orthotopic mouse model of pancreatic cancer.

After the operating area was disinfected with 70% alcohol, a 1-cm longitudinal cut was made around 3 mm off the midline of an anesthetized C57BL/6 mouse using ketamine/xylazine (100/10 mg/Kg). Then, the exposed pancreas was injected with $2.0x10^6$ luciferase-transfected murine pancreatic cancer cells CRL2460 and the wound was closed using double layer suturing. The animal was recovered from anesthetization, and meloxicam was administered via subcutaneous injection (2mg/Kg) every 12 hours for the next two days.

In vivo and ex vivo Imaging.

Seven to ten days after cell injection, the progress of tumor growth was monitored by bioluminescence imaging (Xenogen IVIS 200) after treating mice with an intraperitoneal dose of D-luciferin (150 µg/g). To test the specificity of the TFNS nanoparticles, a 1.5-cm sharp cut was made on the abdomen, and the exposed pancreas was sprayed with TFNS nanoparticles (2mg/Kg, 100 µL) for 5 minutes. Then, imaging was initiated after a careful wash with PBS (1x) to remove unbound probe using the GFP channel. For ex vivo imaging, the pancreas was subsequently dissected along with a portion of muscle from the thigh and sprayed with TFNS nanoparticles for 5 min followed by imaging after a thorough wash with 1X PBS.

Immunohistochemistry.

After fluorescent imaging using a microscope, human tissues were snap frozen in OCT (Tissue-Tek, Fisher Scientific) and stored for future use at -80°C. Tissues were sectioned into 8-µm slides using a cryostat (Tissue-Tek Cryo3) and stained with a 1:100 dilution of anti-TF antibodies (LifeSpan BioScience) overnight at 4°C using a sandwich approach. After a brief wash with PBS (1X), slide tissues were treated with secondary biotinylated-labeled antibodies (Vectastain) for 30 minutes. The slides were then treated with ABC reagent (Vectastain Elite ABC kit) for 30 minutes, after which DAB was added for color development. The slides were examined using white light microscopy (Carl Zeiss, Microimaging Inc.).

Quantitative analysis of fluorescence.

After imaging TF expression in the freshly isolated human colonic tissues using fluorescent microscopy, histogram analysis of the TF expression images was conducted using an algorithm developed within MATLAB (MathWorks, Inc., USA). Mean signal intensities of the green color channel were calculated within the region-of-interest (ROI) of the tissue sample and corrected by subtracting the mean signal of the background ROI (i.e. no tissue).

Statistical analysis

Data was presented as mean ± SD. Comparison between the 2 groups was performed using a Student t-test, while a one-way ANOVA (GraphPad software) was used to compare more than 2 groups. In both cases, the significance was set at 95% of confidence.

RESULTS

Multimodal TFNS nanoparticles can be developed reproducibly

Over the years, we have optimized the syntheses of the PNA-laden TFNS nanoparticles through the production and iterative improvement of several batches each year. The quantitative analysis data from this work is validated from 30 batches of syntheses. Unerring stability was characterized and confirmed during this period of time using different analytical techniques (Table 1). The intended topical use of the TFNS nanoparticles is manifested by its large overall size, ranging from 330-350 nm with strong fluorescence emanated from spherical shapes (Fig. 3).

Table 1. Physical properties of the PNA-laden TFNS nanoparticles and techniques of characterization.

Physical Properties	Measured Values (Mean ± SE, n=27)
Overall size [a] (nm)	329 ± 17
Immobilized PNA [b] (μg/mg)	3.4 ±0.3
Fluorescent Intensity [c] (AU)	29730 ± 1696
Zeta potential	- 26.0 mV
Encapsulated Dyes [d]	0.05%
Thickness of Coating Polymers (PMAA+PNVA) [e] (nm)	15
Polymer Ratio (Polystyrene:PNVA:PMAA) [f]	1300:3:1
Branching Numbers (Vinyl/Methacrylic acid) [g]	76/55
Average Molecular Weight of PNVA (Mw/Mn) [h]	19668±276/6145 ± 28
Average Molecular Weight of PMAA (Mw/Mn) [i]	29247±2522/21633 ± 1982

[a] TEM, SEM, DLS; [b] Ninhydrin assay; [c] UV-vis; [d] UV-vis; [e] XPS, ^{1}H-NMR; [f] GPC, ^{1}H-NMR; [g] GPC, ^{1}H-NMR; [h] GPC; [i] GPC.

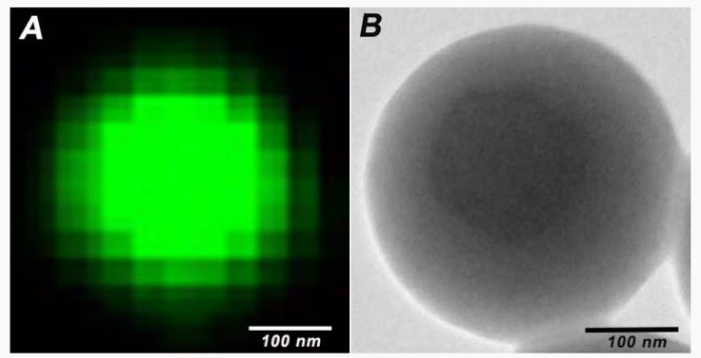

Figure 3. *Imaging data of the TFNS nanoparticles. The overall size and shape of the probe were imaged via high-resolution Airy scan fluorescence microscopy (A) and transmission electron microscopy (B).*

The overall size of the TFNS nanoparticles is dictated mostly by polystyrene with a dominant contributing ratio compared to the other two polymers. The egregious multivalency of nanotechnology was exploited in this work, where approximately 200-300 PNA molecules were fabricated on the surface via the free carboxylic groups of PMAA polymers; while the inner core shelters a large number of coumarin 6 as a signal readout, equivalent to 0.05% by weight. Aside from PMAA, NVA polymers were coated on the surface to reduce non-specific interaction of the probes on the epithelial tissues as we reported previously [31-32]. Overall, both polymers constitute a thin, albeit crucial layer (15 nm) alluding to the enhanced specificity of the probe.

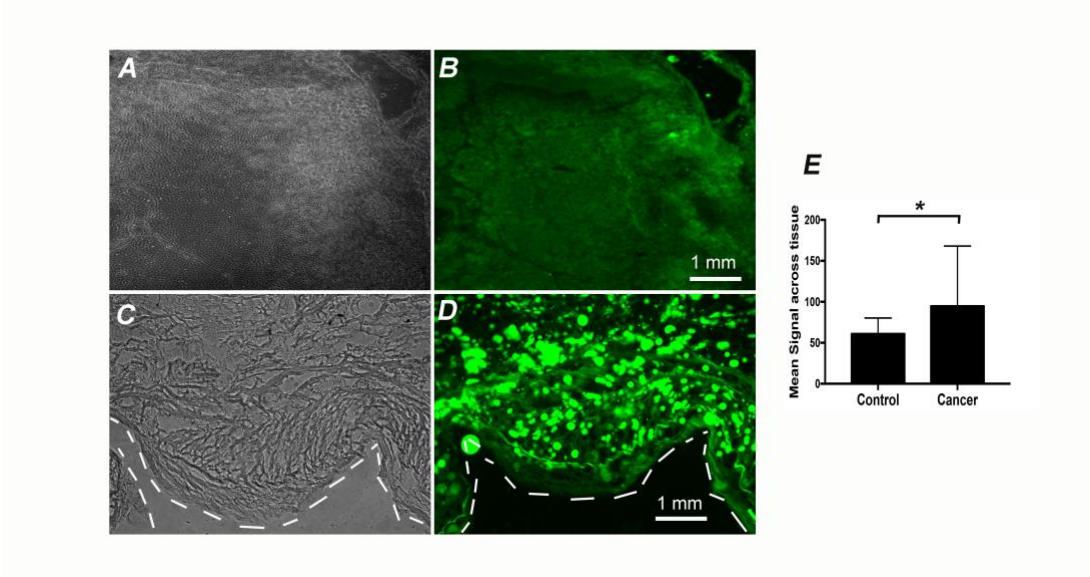

Figure 4. *Specificity of the TFNS nanoparticles for the detection of pancreatic adenocarcinoma/adenoma specimens. Representative fluorescence imaging data of normal (n=12; A, B) and cancer (n=8; C, D) tissues after a brief treatment of the TFNS nanoparticles (2mg/Kg), followed by washing and observation of the fluorescence signal via a fluorescence microscope. Signal intensity across the tissues was quantified and presented in bar graph (E); * p<0.05*

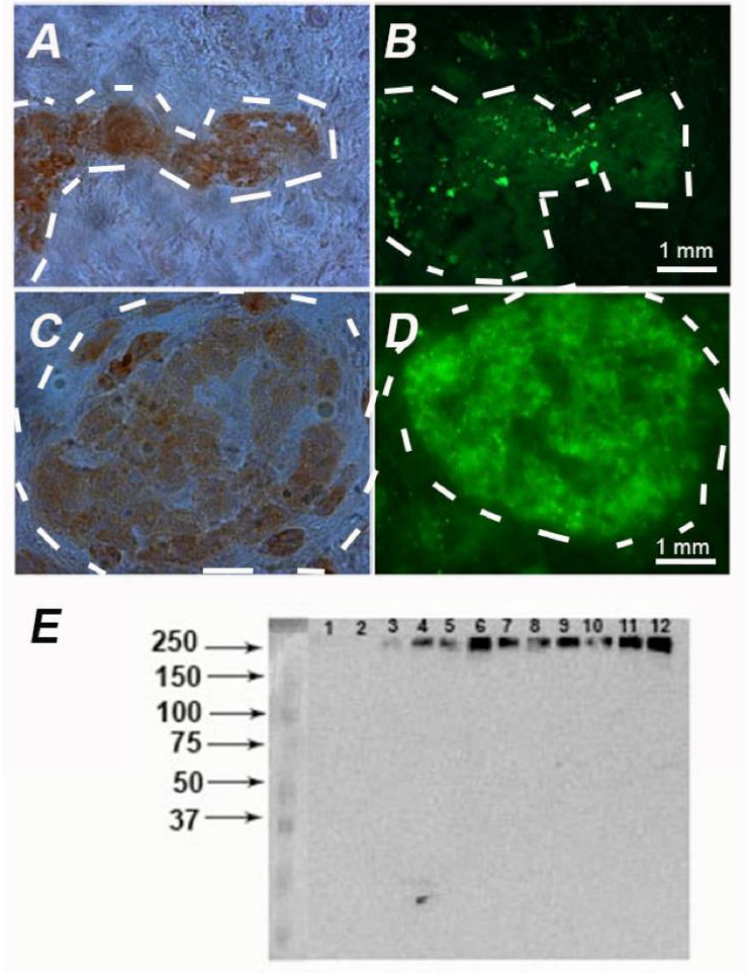

Figure 5. *Delineation of the margin of TF-associated pancreatic cancer. Representative immunohistochemical staining of TF antigen on different human cancer specimens (A, C). Consecutive slides were stained with TFNS nanoparticles (B,D). Western blot analysis of the specimens via immunoprecipitation to detect TF band of approximately 250 KDa; 1, 2 are normal human pancreatic tissues; 3 is benign tissue; 4-12 are malignant tissues.*

TFNS nanoparticles can detect pancreatic cancer with high specificity.

The specificity of the TFNS nanoparticles for the detection of pancreatic cancer was demonstrated in human specimens, cancer vs normal (n=12 normal, n=8 adenocarcinoma/ carcinoma tissues). As shown in Fig. 4, the signal depicted from the TFNS nanoparticles on pancreatic cancer is stronger and more distinguished than those found on normal tissues.

Quantitatively, Matlab analysis using an in-house developed algorithm to analyze the total fluorescence across the tissues indicated that the signals are always stronger in cancer compared to those from normal tissues ($p<0.05$) (Fig. 4E). Most importantly, the data of this work suggested that the probe reflected the tumor margin very consistently as compared to consecutive slides observed under a white light mode.

TFNS nanoparticles detect TF expression on pancreatic cancer.

Next, we wanted to confirm that the fluorescence signal depicted from pancreatic cancer specimens was caused by direct binding between PNA moieties on the surface of TFNS nanoparticles and TF antigens on cancer tissues. Adenocarcinoma/carcinoma slides were prepared and imaged with the TFNS nanoparticles, while the other consecutive slides were stained with anti-TF antibodies. As shown in Fig. 5, the fluorescent signal from the TFNS nanoparticles corroborated those found in the antibody staining, suggesting the recognition of TF antigen on cancer by PNA-laden TFNS nanoparticles. Further, using Western blots of immunoprecipitated antigen, we showed that TF antigen is overexpressed in pancreatic cancer.

In vivo imaging of pancreatic cancer using TFNS nanoparticles.

To demonstrate the specificity of the probe in vivo, we generated an orthotopic mouse model of pancreatic cancer. Toward that approach, human pancreatic cancer cells CRL2460 were stably transfected with luciferase to enable tracking the progress of tumor growth (Fig. 6A).

The cells were operatively injected into the pancreas of wild type mice and the rate of tumor growth was monitored non-invasively in vivo using the Xenogen IVIS optical imaging system (Fig. 6B). The data suggest that the tumor was successfully developed and luciferase-based imaging was effective for monitoring tumor growth. To test the specificity of the topically applied TFNS nanoparticles, pancreatic tumor was exposed to the probe followed by a brief wash to reduce unspecific binding, then the animals were imaged using GFP excitation/emission channels. Overall, the data demonstrated the specificity of the probe both in in vivo and ex vivo (Fig. 6C, D).

DISCUSSION

This work showed that the developed PNA-laden TFNS nanoparticles have an unequivocal specificity for TF antigen. They can detect the overexpression of TF antigen and delineate the margin of pancreatic cancer in human specimens using optical methods (Fig.4,5). This is the first report of TFNS nanoparticles for detection of pancreatic cancer, and it sheds more light on our previous observations that PNA-laden nanoparticles can detect TF-associated epithelial-based tumors[30], with no registered toxicity[33].

The TF antigen is a cryptic glycoprotein, and is referred to as a cancer-associated antigen because it is masked by carbohydrates in normal tissues, but present in many human cancers, including gastrointestinal, lung, pancreatic and ovarian carcinomas[34]. Particularly, ductal adenocarcinoma of the pancreas, often known as pancreatic cancer, remains a lethal malignancy with poor prognosis owing to therapeutic resistance and late clinical presentation[35]. Therefore, identifying a biomarker associated with pancreatic cancer is crucial, not only for early detection and/or monitoring the progress/ response during therapy, but most importantly, for the ability to delineate tumor margins, as surgical dissection of pancreatic cancer increases survival rate for the patients[36-38]. However, 50% to over 80% of patients with pancreatic cancer may develop cancer relapse because of the lack of correct tumor margin detection during resection[39].

In the very first step toward improving margin detection, we wondered whether TF antigen is exclusively expressed also in pancreatic cancer when compared to normal tissue, as we have

observed in colorectal cancer [30]. As shown in Fig.4, TFNS nanoparticles light up pancreatic cancer with a remarkable fluorescence signal. In contrast, no comparable degree of signal intensity is detected in normal tissue other than the usual autofluorescence, given coumarin 6 dyes used in this probe is a visible dye. This is a typical limitation for imaging in the visible spectrum; the future modification of the probes using near-infrared dyes would certainly rectify this issue. Nevertheless, quantitative signal analysis across the tissues of all tested samples proved that the mean signal intensity of the tumor is always higher than those of normal tissue ($P<0.05$) (Fig. 4E). The variance of the fluorescence signal in tumor is high, suggesting the heterogenous expression of TF antigen on pancreatic cancer; and this observation corroborates TF immunohistochemistry data (Fig. 5).

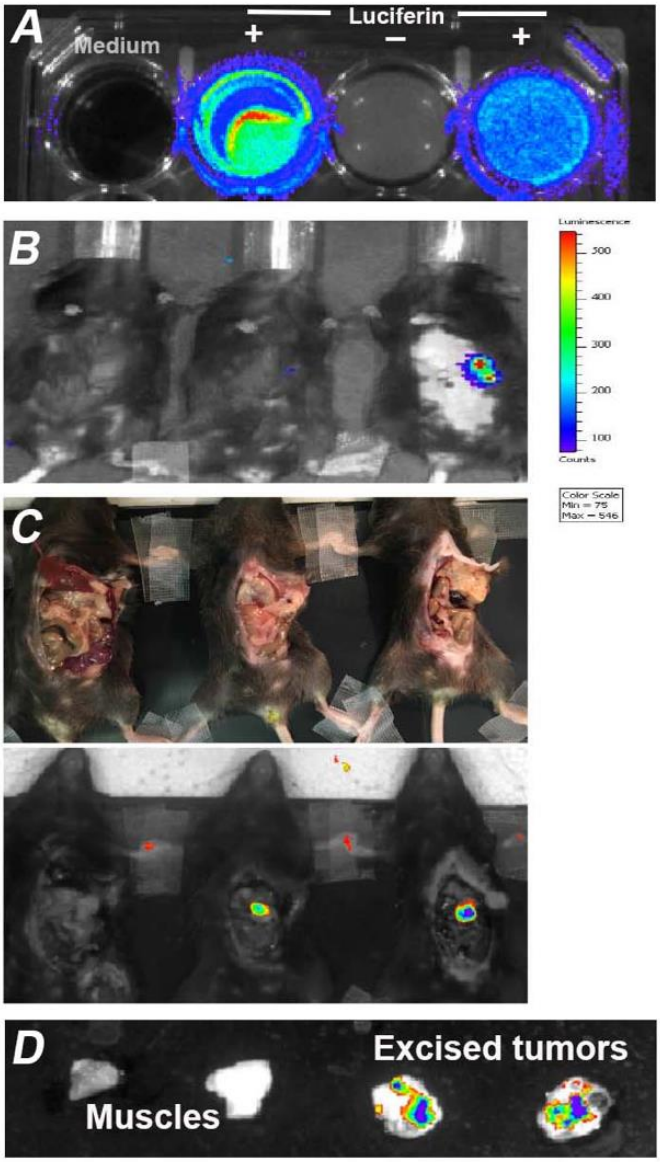

Figure 6. *Orthotopic mouse model of pancreatic cancer and in vivo imaging using the TFNS nanoparticles. Murine pancreatic cancer cells CRL2460 were transfected with luciferase and confirmed via bioluminescence imaging after treatment with luciferin (A); Tumor model was generated using wt mice and the progress of tumor growth was confirmed non-invasively via bioluminescence. Mouse on the left is tumor-free. The mouse in the center and right bore pancreatic tumor, albeit only the animal on the right showed luminescence signal in an intact imaging operation (B); In vivo imaging of exposed pancreatic tumor, in which all three mice were briefly sprayed with the TFNS nanoparticles, washed and imaged using the IVIS optical system (C); Ex-vivo imaging of dissected tumor against control tissues obtain from muscles (D).*

Further, in vivo imaging using an orthotopic mouse model of pancreatic cancer demonstrated the specificity of the probe, albeit with the caveat that the tissues must be exposed invasively. Since optical imaging has limited tissue penetration, we do not anticipate using this technology for non-invasive detection of pancreatic cancer but rather find it perfectly suitable for use in combination with fluorescence laparoscopy. For all of these purposes, we designed the TFNS nanoparticles as a topical imaging agent, which seems ideal for this case since unlike other imaging targets that require the probes to remain intact through systemic delivery, TF antigen is expressed on the surface of epithelial cells, thus localized, topical delivery can be implemented to improve the efficiency of the targeting agent. In addition, its substantially large size and accessibility at the cell surface coupled with the occurrence of tandem repeated regions of MUC1 protein backbone, help to amplify the targeting signal.

CONCLUSIONS

In conclusion, based on our data, it is certain that high expression of TF antigen in pancreatic cancer and its absence from normal tissue represents a unique association in pancreatic carcinoma that exhibits the qualities of a biomarker for tumor margin delineation. There remain a few notable caveats. Although we tested a very low dose of the TFNS probe, well below the threshold to be considered causing concerns[40], the presence of PNA in the design may limit its application, particularly for patients with peanut allergy.

ACKNOWLEDGEMENTS.

This work was partially funded by R01CA160700 (W.P.), VICC Cancer Center Support Grant (W.P.), Vanderbilt VICTR grant and NIGMS Medical Scientist Training Program T32GM007347. Confocal imaging and analyses were performed in part through the use of the Vanderbilt Cell Imaging Shared Resource supported by 1S10RR027396-01 and 1S10OD021630-01 grants.

BIBLIOGRAPHY

1. Khanal, N.; Upadhyay, S.; Dahal, S.; Bhatt, V. R.; Silberstein, P. T., Systemic therapy in stage IV pancreatic cancer: a population-based analysis using the National Cancer Data Base. *Ther Adv Med Oncol* **2015,** *7* (4), 198-205.

2. Fujiwara, Y.; Suzuki, F.; Kanehira, M.; Futagawa, Y.; Okamoto, T.; Yanaga, K., Radical resection of T1 pancreatic adenocarcinoma with a pseudocyst of the tail due to acute obstructive pancreatitis: report of a case. *Surg Case Rep* **2016,** *2* (1), 144.

3. Ezzati, M.; Henley, S. J.; Lopez, A. D.; Thun, M. J., Role of smoking in global and regional cancer epidemiology: current patterns and data needs. *Int J Cancer* **2005,** *116* (6), 963-71.

4. Hidalgo, M., Pancreatic cancer. *N Engl J Med* **2010,** *362*, 1605-1617.

5. Parkin, D. M.; Boyd, L.; Walker, L. C., 16. The fraction of cancer attributable to lifestyle and environmental factors in the UK in 2010. *Br J Cancer* **2011,** *105 Suppl 2*, S77-81.

6. Willett, W. C., Diet and cancer. *Oncologist* **2000,** *5*, 393-404.

7. Ilic, M.; Ilic, I., Epidemiology of pancreatic cancer. *World J Gastroenterol* **2016,** *22*, 9694-9705.

8. Verbeke, C. S.; Menon, K. V., Redefining resection margin status in pancreatic cancer. *HPB (Oxford)* **2009,** *11* (4), 282-9.

9. Bachmann, J.; Michalski, C. W.; Martignoni, M. E.; Buchler, M. W.; Friess, H., Pancreatic resection for pancreatic cancer. *HPB (Oxford)* **2006,** *8* (5), 346-51.

10. Eberlin, L. S.; Margulis, K.; Planell-Mendez, I.; Zare, R. N.; Tibshirani, R.; Longacre, T. A.; Jalali, M.; Norton, J. A.; Poultsides, G. A., Pancreatic Cancer Surgical Resection Margins: Molecular Assessment by Mass Spectrometry Imaging. *PLoS Med* **2016,** *13* (8), e1002108.

11. Imamura, M.; Doi, R.; Imaizumi, T.; Funakoshi, A.; Wakasugi, H.; Sunamura, M.; Ogata, Y.; Hishinuma, S.; Asano, T.; Aikou, T.; Hosotani, R.; Maetani, S., A randomized multicenter trial comparing resection and radiochemotherapy for resectable locally invasive pancreatic cancer. *Surgery* **2004,** *136* (5), 1003-11.

12. Verbeke, C. S.; Leitch, D.; Menon, K. V.; McMahon, M. J.; Guillou, P. J.; Anthoney, A., Redefining the R1 resection in pancreatic cancer. *Br J Surg* **2006,** *93* (10), 1232-7.

13. Hounsell, E. F.; Davies, M. J.; Renouf, D. V., O-linked protein glycosylation structure and function. *Glycoconjugate journal* **1996,** *13* (1), 19-26.

14. Springer, G. F., T and Tn, General Carcinoma autoantigens. *Science* **1984,** *224*, 1198-1206.

15. Cao, Y.; Stosiek, P.; Springer, G. F.; Karsten, U., Thomsen-Friedenreich-related carbohydrate antigens in normal adult human tissues: a systematic and comparative study. *Histochem Cell Biol* **1996,** *106* (2), 197-207.

16. severino, P. F.; Carrascal, M. A.; Gouveia, H.; Cabral, M. G.; Correia, M.; Malagolini, N.; Chiricolo, M.; Dall'Olio, F.; Videira, P. A., Contribution of Thomsen-Friedenreich antigens to bladder cancer malignancy: Characterization of cell line models. *BMC Proc.* **2010,** *4*, p48.

17. Brockhausen, I., Mucin-type O-glycans in human colon and breast cancer: glycodynamics and functions. *EMBO Rep* **2006,** *7* (6), 599-604.

18. Baldus, S. E.; Zirbes, T. K.; Glossmann, J.; Fromm, S.; Hanisch, F. G.; Monig, S. P.; Schroder, W.; Schneider, P. M.; Flucke, U.; Karsten, U.; hiele, J.; Holscher, A. H.; Dienes, H. P., Immunoreactivity of monoclonal antibody BW835 represents a marker of progression and prognosis in early gastric cancer. *Oncology* **2001,** *61* (2), 147-55.

19. Slovin, S. F.; Ragupathi, G.; Musselli, C.; Fernandez, C.; Diani, M.; Verbel, D.; Danishefsky, S.; Livingston, P.; Scher, H. I., Thomsen-Friedenreich (TF) antigen as a target for prostate cancer vaccine: clinical trial results with TF cluster (c)-KLH plus QS21 conjugate vaccine in patients with biochemically relapsed prostate cancer. *Cancer Immunol Immunother* **2005,** *54* (7), 694-702.

20. Glinskii, O. V.; Sud, S.; Mossine, V. V.; Mawhinney, T. P.; Anthony, D. C.; Glinsky, G. V.; Pienta, K. J.; Glinsky, V. V., Inhibition of prostate cancer bone metastasis by synthetic TF antigen mimic/galectin-3 inhibitor lactulose-L-leucine. *Neoplasia* **2012,** *14* (1), 65-73.

21. MacLean, G. D.; Bowen-Yacyshyn, M. B.; Samuel, J.; Meikle, A.; Stuart, G.; Nation, J.; Poppema, S.; Jerry, M.; Koganty, R.; Wong, T.; et al., Active immunization of human ovarian cancer patients against a common carcinoma (Thomsen-Friedenreich) determinant using a synthetic carbohydrate antigen. *J Immunother (1991)* **1992,** *11* (4), 292-305.

22. Stein, R.; Chen, S.; Grossmann, W.; Goldemberg, D. M., Human lung carcinoma monocolonal antibody specific for the Thomsen-Friedenreich Antigen *Cancer Res.* **1989,** *49*, 32-37.

23. Shamsuddin, A. M.; Tyner, G. T.; Yang, G. Y., Common Expression of the Tumor Marker d-Galactose-β-[1→3]-N-Acetyl-d-Galactosamine by Different Adenocarcinomas: Evidence of Field Effect Phenomenon. *Cancer Research* **1995,** *55*, 149-152.

24. Ueno, E.; Otsuka, K.; Kudo, T.; Ohkuma, S., Isolation and characterization of a Vicia graminea and Vicia unijuga lectins-binding (Vgu) glycoprotein with Thomsen-Friedenreich (T) activity from human liver metastases of pancreas carcinoma. *Int J Biochem* **1992,** *24* (5), 769-76.

25. Springer, G. F.; Desai, P. R.; Fry, W. A.; Goodale, R. L.; Shearen, J. G.; Scanlon, E. F., **1983.** *Cancer Detect Prev* T antigen, a tumor marker against which breast, lung and pancreas carcinoma patients mount immune responses, (6), 111-8.

26. Hakamory, S., Tumor-associated carbohydrate antgigens defining tumor malignancy. *The Molecular Immunology of Complex Carbohydrates-2, Kluwer Academic/Plenum Publishing* **2001**, 369-402.

27. Yuan, M.; Itzkowitz, S. H.; Boland, C. R.; Kim, Y. D.; Tomita, J. T.; Palekar, A.; Bennington, J. L.; Trump, B. F.; Kim, Y. S., Comparison of T-antigen expression in normal, premalignant, and malignant human colonic tissue using lectin and antibody immunohistochemistry. *Cancer Res* **1986,** *46* (9), 4841-7.

28. Muller, C. B.; Enderlein, J., Image Scanning Microscopy. *Phys Rev Lett* **2010,** *104*, 198101.

29. Huff, J., The Airyscan detector from ZEISS: confocal imaging with improved signal-to-noise ratio and superresolution. *Nat Methods* **2015,** *12*, 1205.

30. Kumagai, H.; Pham, W.; Kataoka, M.; Hiwatari, K.; McBride, J.; Wilson, K. J.; Tachikawa, H.; Kimura, R.; Nakamura, K.; Liu, E. H.; Gore, J. C.; Sakuma, S., Multifunctional nanobeacon for imaging Thomsen-Friedenreich antigen-associated colorectal cancer. *Int J Cancer* **2013,** *132* (9), 2107-17.

31. Sakuma, S.; Sudo, R.; Suzuki, N.; Kikuchi, H.; Akashi, M.; Hayashi, M., Mucoadhesion of polystyrene nanoparticles having surface hydrophilic polymeric chains in the gastrointestinal tract. *Int J Pharm* **1999,** *177* (2), 161-72.

32. Sakuma, S.; Sudo, R.; Suzuki, N.; Kikuchi, H.; Akashi, M.; Ishida, Y.; Hayashi, M., Behavior of mucoadhesive nanoparticles having hydrophilic polymeric chains in the intestine. *J Control Release* **2002,** *81* (3), 281-90.

33. Sakuma, S.; Kumagai, H.; Shimosato, M.; Kitamura, T.; Mohri, K.; Ikejima, T.; Hiwatari, K.; Koike, S.; Tobita, E.; McClure, R.; Gore, J. C.; Pham, W., Toxicity studies of coumarin 6-encapsulated polystyrene nanospheres conjugated with peanut agglutinin and poly(N-vinylacetamide) as a colonoscopic imaging agent in rats. *Nanomedicine* **2015,** *11* (5), 1227-36.

34. Hassanein, A. M.; Al-Quran, S. Z.; Kantor, G. R.; Pauporte, M.; Telang, G. H.; Spielvogel, R. L., Thomsen-Friedenreich (T) antigen: a possible tool for differentiating sebaceous carcinoma from its simulators. *Appl Immunohistochem Mol Morphol* **2001,** *9* (3), 250-4.

35. Verbeke, C. S., Resection margins in pancreatic cancer. *Pathologe* **2013,** *34*, 241-47.

36. Neoptolemos, J. P.; Stocken, D. D.; Dunn, J. A.; Almond, J.; Beger, H. G.; Pederzoli, P.; Bassi, C.; Dervenis, C.; Fernandez-Cruz, L.; Lacaine, F.; Buckels, J.; Deakin, M.; Adab, F. A.; Sutton, R.; Imrie, C.; Ihse, I.; Tihanyi, T.; Olah, A.; Pedrazzoli, S.; Spooner, D.; Kerr, D. J.; Friess, H.; Buchler, M. W., Influence of resection margins on survival for patients with pancreatic cancer treated by adjuvant chemoradiation and/or chemotherapy in the ESPAC-1 randomized controlled trial. *Ann Surg* **2001,** *234* (6), 758-68.

37. Sohn, T. A.; Yeo, C. J.; Cameron, J. L.; Koniaris, L.; Kaushal, S.; Abrams, R. A.; Sauter, P. K.; Coleman, J.; Hruban, R. H.; Lillemoe, K. D., Resected adenocarcinoma of the pancreas-616 patients: results, outcomes, and prognostic indicators. *J Gastrointest Surg* **2000,** *4* (6), 567-79.

38. Willett, C. G.; Lewandrowski, K.; Warshaw, A. L.; Efird, J.; Compton, C. C., Resection margins in carcinoma of the head of the pancreas. Implications for radiation therapy. *Ann Surg* **1993,** *217* (2), 144-8.

39. Griffin, J. F.; Smalley, S. R.; Jewell, W.; Paradelo, J. C.; Reymond, R. D.; Hassanein, R. E.; Evans, R. G., Patterns of failure after curative resection of pancreatic carcinoma. *Cancer* **1990,** *66* (1), 56-61.

40. Ryder, S. D.; Smith, J. A.; Rhodes, J. M., Peanut lectin: a mitogen for normal human colonic epithelium and human HT29 colorectal cancer cells. *Journal of the National Cancer Institute* **1992,** *84* (18), 1410-6.

Quote as: Barton S, Li B, Siuta M, Janve VA, Song J, Holt CM, Tomono T, Ukawa M, Kumagai H, Tobita E, Wilson K, Sakuma S, Pham W. Specific Molecular Recognition as a Strategy to Delineate Tumor Margin Using Topically Applied Fluorescence Embedded Nanoparticles, Prec. Nanomed. 2018 Oct;1(3):197-210 DOI:10.29016/181027.1